JOURNAL OF BACTERIOLOGY, May 1995, p. 2387–2395 Vol. 177, No. 9
0021-9193/95/$04.00+0

Envelope Structure of Four Gliding Filamentous Cyanobacteria

EGBERT HOICZYK AND WOLFGANG BAUMEISTER*
Max-Planck-Institut für Biochemie, D-82152 Martinsried, Germany

Received 14 November 1994/Accepted 24 February 1995

The cell walls of four gliding filamentous *Oscillatoriaceae* species comprising three different genera were studied by freeze substitution, freeze fracturing, and negative staining. In all species, the multilayered gram-negative cell wall is covered with a complex external double layer. The first layer is a tetragonal crystalline S-layer anchored on the outer membrane. The second array is formed by parallel, helically arranged surface fibrils with diameters of 8 to 12 nm. These fibrils have a serrated appearance in cross sections. In all cases, the orientation of the surface fibrils correlates with the sense of revolution of the filaments during gliding, i.e., clockwise in both *Phormidium* strains and counterclockwise in *Oscillatoria princeps* and *Lyngbya aeruginosa*. The lack of longitudinal corrugations or contractions of the surface fibrils and the identical appearances of motile and nonmotile filaments suggest that this structure plays a passive screw thread role in gliding. It is hypothesized that the necessary propulsive force is generated by shear forces between the surface fibrils and the continuing flow of secreted extracellular slime. Furthermore, the so-called junctional pores seem to be the extrusion sites of the slime. In motile cells, these pores exhibit a different staining behavior than that seen in nonmotile ones. In the former, the channels of the pores are filled with electron-dense material, whereas in the latter, the channels appear comparatively empty, highly contrasting the peptidoglycan. Finally, the presence of regular surface structures in other gliding prokaryotes is considered an indication that comparable structures are general features of the cell walls of gliding microbes.

Many multicellular, filamentous cyanobacteria move on solid surfaces by a type of motility described as gliding. Gliding is not exclusive to cyanobacteria but rather is widespread among prokaryotes (for a review, see references 3 and 20). It is unknown whether gliding motility is in all cases based on a common mechanism.

Gliding of the nonpolar, filamentous cyanobacteria appears as a slow uniform motion, occasionally interrupted by reversals (13). Neither wriggling nor contraction nor peristaltic alterations of the filamentous trichomes are detectable by light microscopy (38). Members of the *Oscillatoriaceae* translocate in a highly coordinated manner. Translational movements are accompanied in most species by revolution around the long axis of the filament (4). While moving, the trichomes secrete slime which is left behind as a twisted and collapsed thin tube (20). The sense of revolution is unique and species specific (46), as evinced by the handedness of the rotation.

The lack of flagella or of other plausible locomotive organelles is puzzling. Electron microscopic studies have so far failed to identify motor structures common among gliders. A number of unusual structures have been described which may or may not be related to this peculiar type of motility. This list comprises spinning discs (37), fibrils within the cell or the cell wall (2, 47), chain-like strands (31), anchorage sites of the cell surface (29), contractile surface appendages (33), cellular inclusions (rhapidosomes) (9), and extruded extracellular material (10, 41).

Halfen and Castenholz (23) described a "locomotory machinery" which is assembled from parallel fibrils with diameters of 5 to 8 nm, aligned in a helical array just underneath the outer membrane. The correspondence of the fibril arrangement and the helical path of the filaments (21) was taken as an indication that these structures are indeed involved in motility.

* Corresponding author. Mailing address: Molekulare Strukturbiologie, Max-Planck-Institut für Biochemie, D-82152 Martinsried, Germany. Phone: (089) 8575 2652. Fax: (089) 8578 2641.

As the morphological preservation of these putative motor fibrils in thin sections was not satisfactory and the correlation with structures seen in freeze fracture barely possible, we have reinvestigated the envelope structure with recently developed cryotechniques. These techniques provide a much improved structural preservation of the cells (for a review, see references 16, 18, and 24), which is an indispensable prerequisite for the investigation of such delicate structures.

In this communication, we describe the envelope structures of four species of gliding cyanobacteria and discuss them in relation to motility. It is demonstrated that these species, belonging to different genera (*Oscillatoria*, *Phormidium*, and *Lyngbya*), possess identical structures on their trichome surfaces.

MATERIALS AND METHODS

Cyanobacterial strains and culture conditions. *Oscillatoria princeps*, isolated from a canal at Schloß Nymphenburg, Munich, Germany, in May 1991, was grown in 500-ml Erlenmeyer flasks in a mineral medium (5). In addition, two strains of *Phormidium uncinatum* were used, a black-colored strain isolated in Tübingen (35) and a green-colored one from Lake Baikal (14). Both strains differ not only in pigmentation but also in growth, morphology, and motility. *Lyngbya aeruginosa* was obtained from the Göttingen algal culture collection (strain number B47.79). All three species were cultivated on an agar (0.4%) mineral medium (36) under constant white light (800 lx) at a temperature of 20°C.

Sample preparation. All preparation conditions were selected to optimize gliding motility. Immediately before chemical or physical fixation, motility was examined by light microscopy. For all fixation and embedding protocols, filaments were put on cigarette paper (Job no. 807S) and placed in a wet chamber. After 1 or 2 h under appropriate light conditions, the filaments still glide in an undisturbed manner. Ultrathin sections were made only from embedded filaments which were in motion at the time the fixation started.

Conventional fixation. For conventional chemical fixation, the paper with the organisms was immersed in medium containing 2% (vol/vol) glutaraldehyde for 2 h at room temperature. Fixed cells were washed twice with pure medium, postfixed with either 2% (wt/vol) osmium tetroxide alone or a mixture of 2% (wt/vol) osmium tetroxide and 1% ruthenium red (30) in medium for 2 h at room temperature and washed again with medium twice. The filaments on the paper were then dehydrated through a graded acetone series, infiltrated overnight at room temperature in an acetone-Epon 812 mixture (1:1), embedded in fresh Epon 812, and polymerized at 60°C for 36 h.

Freeze substitution. For freeze substitution, the prepared gliding filaments

were immediately cryofixed either by slamming them onto a copper block cooled with liquid helium (11) or by plunging them (4 m s^{-1}) into liquid ethane (8). Substitution was performed in pure acetone containing 2% (wt/vol) osmium tetroxide and a molecular sieve (pore diameter, 0.4 nm) for 80 h at −87°C (see also reference 18). The temperature was gradually increased (11.8°C/h) to −42°C and then to 0°C (10.0°C/h). Excess fixative was removed by washing the samples with pure acetone at room temperature. The samples were infiltrated with acetone-Epon 812 mixtures (2:1 for 1 h, 1:1 for 1 h, and 1:2 overnight with opened covers to allow the acetone to evaporate), transferred into fresh pure Epon 812 for 3 h, embedded, and polymerized at 60°C for 36 h.

Cryofixed samples were dehydrated in acetone containing 0.3% uranyl acetate, 3% glutaraldehyde, and a molecular sieve (for complete dehydration) for 80 h at −87°C. The temperature was then increased to −42°C (8.0°C/h) and held constant for 6 h. The samples were washed with pure acetone at the same temperature and infiltrated with acetone-Lowicryl (HM 23) mixtures (1:1 for 75 min and 1:2 for 2 h), embedded in pure Lowicryl for 2 h, and polymerized by UV radiation for 24 h at −42°C and for 80 h at room temperature.

Some samples were cryosubstituted with diethyl ether containing 2% (wt/vol) osmium tetroxide and a molecular sieve at −85°C for 21 days. The tubes with the samples were placed in a massive two-part cylindrical aluminum block (diameter, 12 cm, and height, 16 cm) that had central holes and that was cooled to −87°C. After substitution, the blocks containing the samples were placed in an insulation jacket and slowly warmed up to room temperature (2.0°C/h). The samples were washed with pure diethyl ether and infiltrated with diethyl ether-Spurr mixtures, transferred into pure Spurr medium, and polymerized at 70°C overnight.

Freeze fracturing. Filaments were processed for freeze fracturing and etching according to standard protocols. Briefly, the filaments were infiltrated stepwise with glycerol (25%), mounted between copper sandwiches, and frozen with a propane jet (Cryo-jet QFD 101; Balzers). Alternatively, motile filaments on cigarette paper were frozen by plunging or slamming them without fixation or cryoprotection. The latter samples were glued on top of a drop of butylbenzene at −80°C and fractured with a knife. Freeze fracturing was performed with a Balzers BA 360 unit at −115°C. After the samples were etched for 1 to 3 min, carbon-platinum was deposited unidirectionally at an angle of 45° and the replicas were reinforced with carbon, cleaned with 70% sulfuric acid, and picked up on 400-mesh copper grids.

Light and electron microscopy. Living trichomes of the different species were examined by means of a light microscope equipped with bright-field, phase contrast, and differential interference contrast optics.

For electron microscopy, thin sections were mounted on Formvar carbon-coated copper grids. Sections were routinely poststained with 2% (wt/vol) uranyl acetate and lead citrate (40). Isolated cell wall layers were negatively stained on glow discharge-treated carbon films with either 2% (wt/vol) uranyl acetate or 1.5% (wt/vol) sodium phosphotungstate at pH 6.8 containing glucose (0.015%) to promote homogeneous staining. For electron microscopy, a Philips CM 10 was used at 100 kV.

Cell wall preparation. Filaments of *P. uncinatum* Baikal harvested by centrifugation were washed twice in 20 mM Tris-HCl (pH 7.4) with 5 mM $MgCl_2$. The cells were then broken in an ice-cooled cell mill (Vibrogen; Bühler) in the presence of DNase II and 20 mM phenylmethylsulfonyl fluoride as a proteinase inhibitor. Crude cell envelopes were obtained by differential centrifugation (5 min at 200 × *g* and 15 min at 10,000 × *g*) and purified with a Percoll density gradient for 1 h at 1,000 × *g*. A pale orange-colored pellet formed at the bottom of the tube, and a broad band of low density appeared at the top of the tube. The former contain purified cell walls, and the latter contained thylakoids and cell debris. To remove the Percoll, the cell walls were washed five times with the Tris-HCl buffer containing $MgCl_2$ and phenylmethylsulfonyl fluoride (48).

RESULTS

Morphology of cell walls in conventional preparations. Thin sections of the cells revealed, for all species investigated in our study, a complex multilayered envelope structure which is characteristic of cyanobacteria (7, 15). Proceeding from inside, the cytoplasmic membrane (about 6 nm) is covered by a peptidoglycan layer of variable thickness (ranging from 10 to 25 nm in *P. uncinatum* and *L. aeruginosa* to 250 to 650 nm in *O. princeps*) and an outer membrane (about 6 nm). The cell envelopes combine gram-positive (thick peptidoglycan) as well as gram-negative (outer membrane) features.

Typically, the outer membranes in all species are highly convoluted, as is often seen in conventionally prepared sections of gram-negative bacteria. Once this appearance was thought to be the consequence of undulating movements of the outer membrane (3), but in fact this seems to be an artifact caused by postmortem shrinkage of the cells during fixation and dehydration. While the spacing observed between the outer membrane and the peptidoglycan layer was relatively constant (maximum, 10 nm), it varied strongly between the peptidoglycan layer and the cytoplasmic membrane (varying from about 0 to 100 nm in all investigated species).

The preservation of the extracellular polysaccharides of the investigated species is rather poor. The slime secreted during gliding is lost during the processes of dehydration and embedding, although the more condensed sheaths of old, nonmotile trichomes are often well preserved, especially when ruthenium red is added to the fixative.

Improved morphology of cell walls after cryosubstitution: a view based upon comparison of freeze-substituted cells with conventionally prepared cells. Envelope profiles of freeze-substituted cells appeared quite different from those of conventionally fixed ones (Fig. 1A, B, C, and D). All the outer membranes show rather straight double-track structures with uniform widths of 6 to 8 nm. At every cross wall, the outer membrane invaginates slightly, forming a junction with the underlying peptidoglycan (Fig. 1E and F). These circumferential junctions resemble the periseptal annuli described for several other eubacteria (32). The junctions separate the part of the periplasmic space between the outer membrane and the peptidoglycan of the single cells within the filaments. They are situated at the midplane between junctional pores (26) which pass through the peptidoglycan from cells on either side of the cross wall. The periplasmic space ranges from 6 to 14 nm and appears homogeneous; it is not translucent, as it is in conventional preparations. The cytoplasmic membrane often appears as a single electron-dense line 3 to 4 nm in width, corroborating the observation that the outer face is tightly pressed against the peptidoglycan and, therefore, difficult to observe (17). On occasion, the cytoplasmic membrane appeared as a double-track profile with a width equal to 6 to 9 nm, with the inner track less densely stained. Obviously, the tight association of the cytoplasmic membrane and the peptidoglycan obtained by cryotechniques seems to represent a more reliable image of the turgid state of the cells.

The electron-dense peptidoglycan has a uniform width ranging from 15 to 30 nm in *L. aeruginosa* up to 35 nm in both *Phormidium* strains and 300 to 700 nm in *O. princeps*. In general, the peptidoglycan was thicker and the structure was more homogeneous in cells prepared by cryotechniques than in those prepared conventionally.

Ultrastructure of the pores of the cell walls. Among the species we have studied, *O. princeps* is the only one that has the large pores (21). These large pores have diameters of up to 350 nm at their bases and center-to-center spacings of ca. 400 nm (Fig. 1C and 2D and E). They are in fact nonpenetrating discontinuities of the peptidoglycan filled with cytoplasm rather than real pores. All four species, however, have the junctional pores described previously by Lamont (26) (Fig. 1E and F and 2D and E). These junctional pores form channels radiating outward from the cytoplasm on opposite sides of the septa at angles of approximately ±30 to ±40° relative to each septum. In all the species, the junctional pores of motile filaments were filled with material of approximately the same electron density as that of the peptidoglycan and, therefore, were barely visible (Fig. 1E and F). The channels of the pores could be easily observed in nonmotile filaments of *O. princeps*, *L. aeruginosa*, and *P. uncinatum* (strain Baikal), in which they appeared as electron-translucent structures (Fig. 2D and E). However, the junctional pores are also present in motile filaments; this could be demonstrated by negative staining of isolated murein sacculi (Fig. 3B). The diameters of the junctional pores are about 14 to 16 nm, while the center-to-center distances are approximately twice the diameter. These dimen-

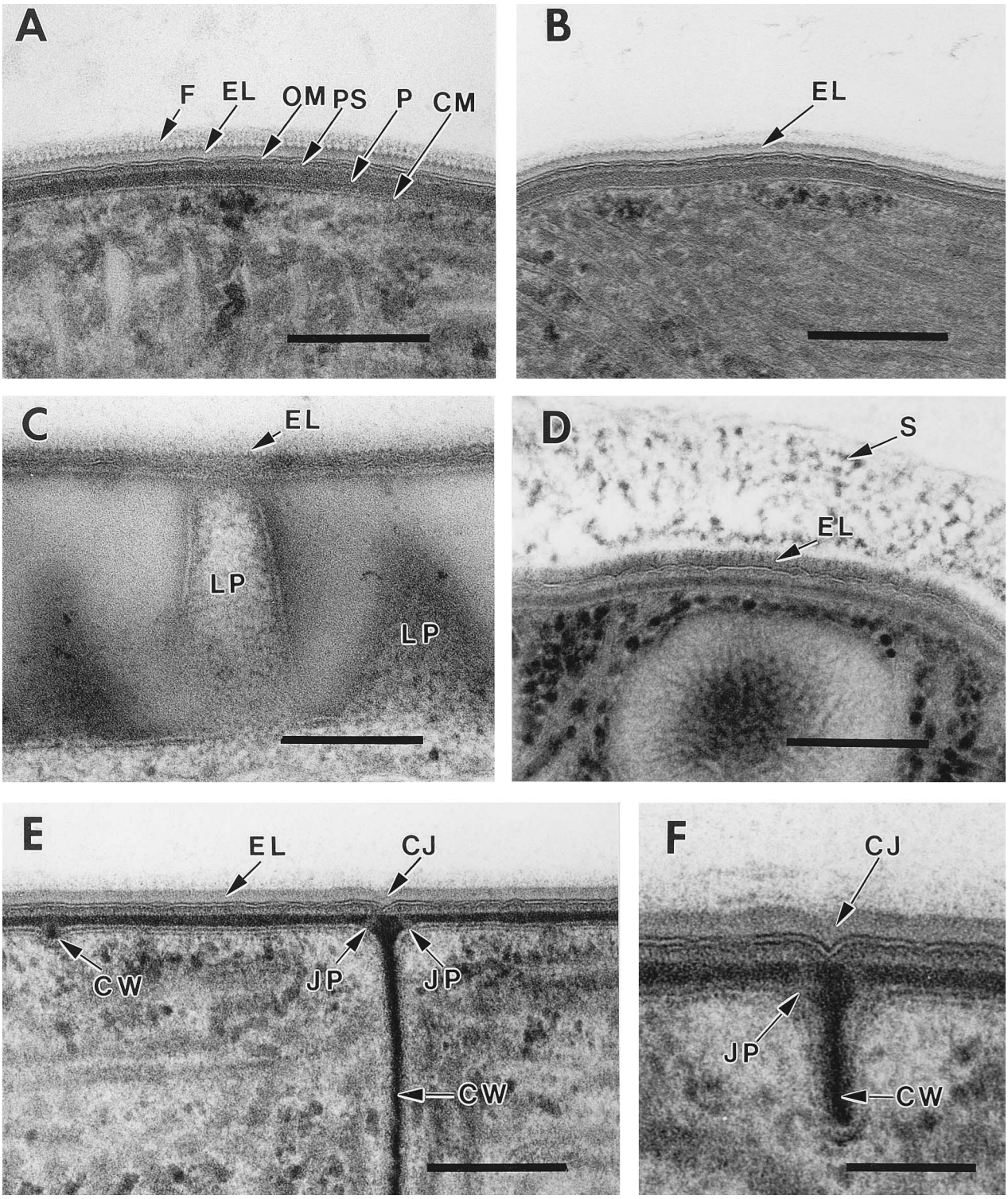

FIG. 1. (A) *P. uncinatum* (strain Tübingen). Cross section of cryosubstituted motile filament showing the complex external layer with its serrated substructure. CM, cytoplasmic membrane; EL, serrated external layer; F, hair-like fibers; OM, outer membrane; P, peptidoglycan; PS, periplasmic space. Bar, 200 nm. (B) *P. uncinatum* (strain Baikal). Cross section of cryosubstituted motile filament with the EL. Bar, 200 nm. (C) *O. princeps*. Cross section of a cryosubstituted motile filament showing the outer pattern of the EL. LP, large pore. Bar, 200 nm. (D) *L. aeruginosa*. Cross section of a cryosubstituted old immobile trichome. The EL is clearly visible, but the serrated substructure is lost. S, sheath. Bar, 200 nm. (E) *P. uncinatum* (strain Tübingen). Longitudinal section showing the multilayered cell wall. The junctional pore (JP) channels are filled with material. At the young cross wall (CW) bud at the left side, the channels start to evaginate. On the outer side, the circumferential junction (CJ) with the outer membrane is still not developed. Bar, 200 nm. (F) *P. uncinatum* (strain Baikal). Longitudinal section showing the CJ at the CW. Bar, 100 nm.

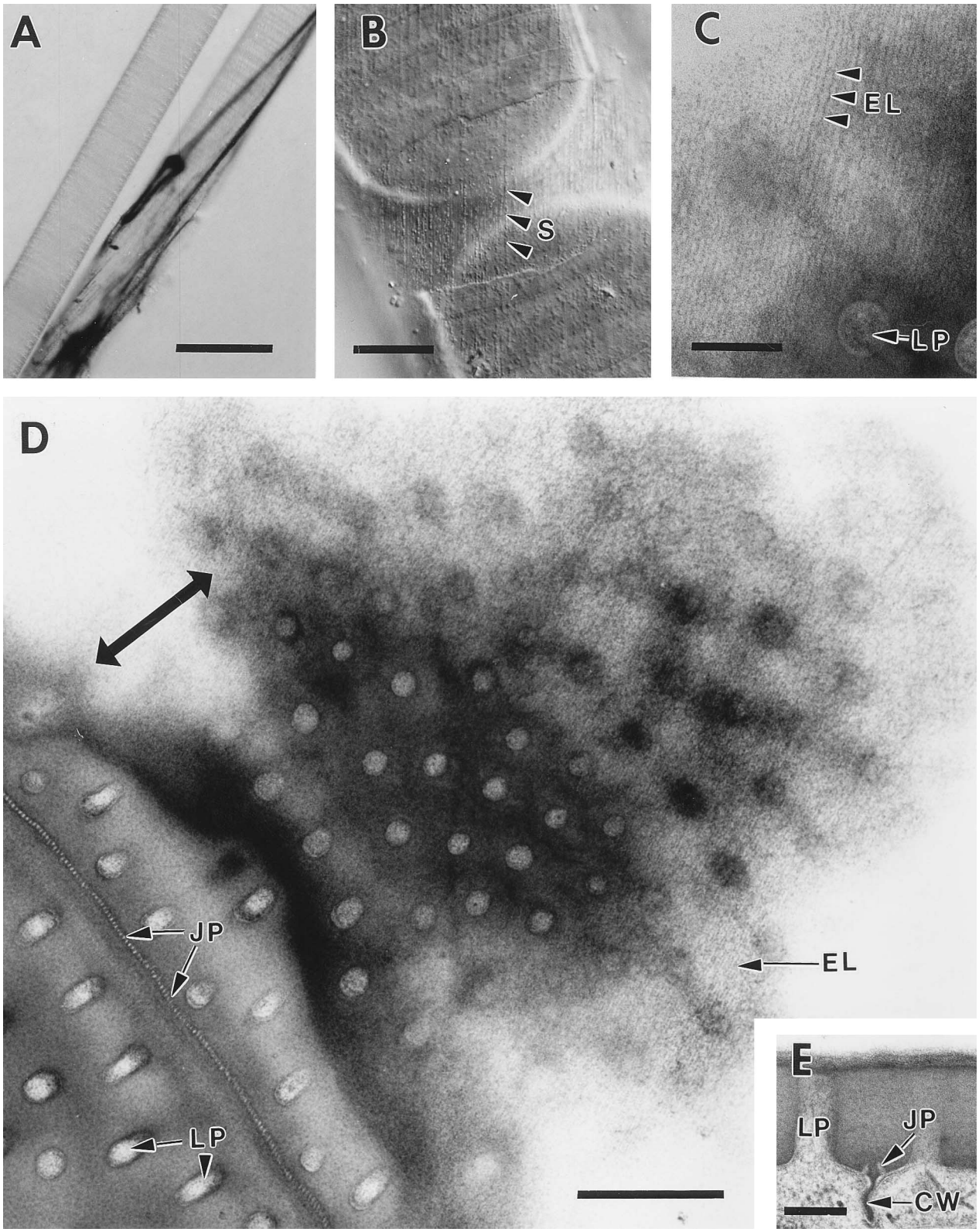

FIG. 2. (A) Light micrograph of filaments of *O. princeps* secreting slime stained with India ink. The slime bands move in a helical pattern along the surface of the trichome, which is suspended in medium. Because of the reversed view of the light microscope, the arrangement of the slime bands is counterclockwise with respect to the cell. Bar, 100 μm. (B) Light micrograph of the sheath of a nonmotile *Oscillatoria* filament (differential interference contrast image). At the surface of the sheath, the helically arranged sheath fibrils (S) are visible. Because of the reversed view of the light microscope, the arrangement of the fibrils is counterclockwise with respect to the cell. Bar, 20μm. (C) *O. princeps*. Tangential section revealing the helical pattern of the serrated periodic surface fibrils (EL). LP, large pore. Bar, 200 nm. (D)*O. princeps*. Tangential section of a nonmotile filament with the EL. The junctional pore (JP) channels possess a high contrast to the murein. The arrangement of the EL is counterclockwise. Note that the orientation of the filament is indicated by the large arrow. Bar, 2 μm. (E) *O. princeps*. Longitudinal section of a developing cross wall (CW) with the JP starting to evaginate. Bar, 200 nm.

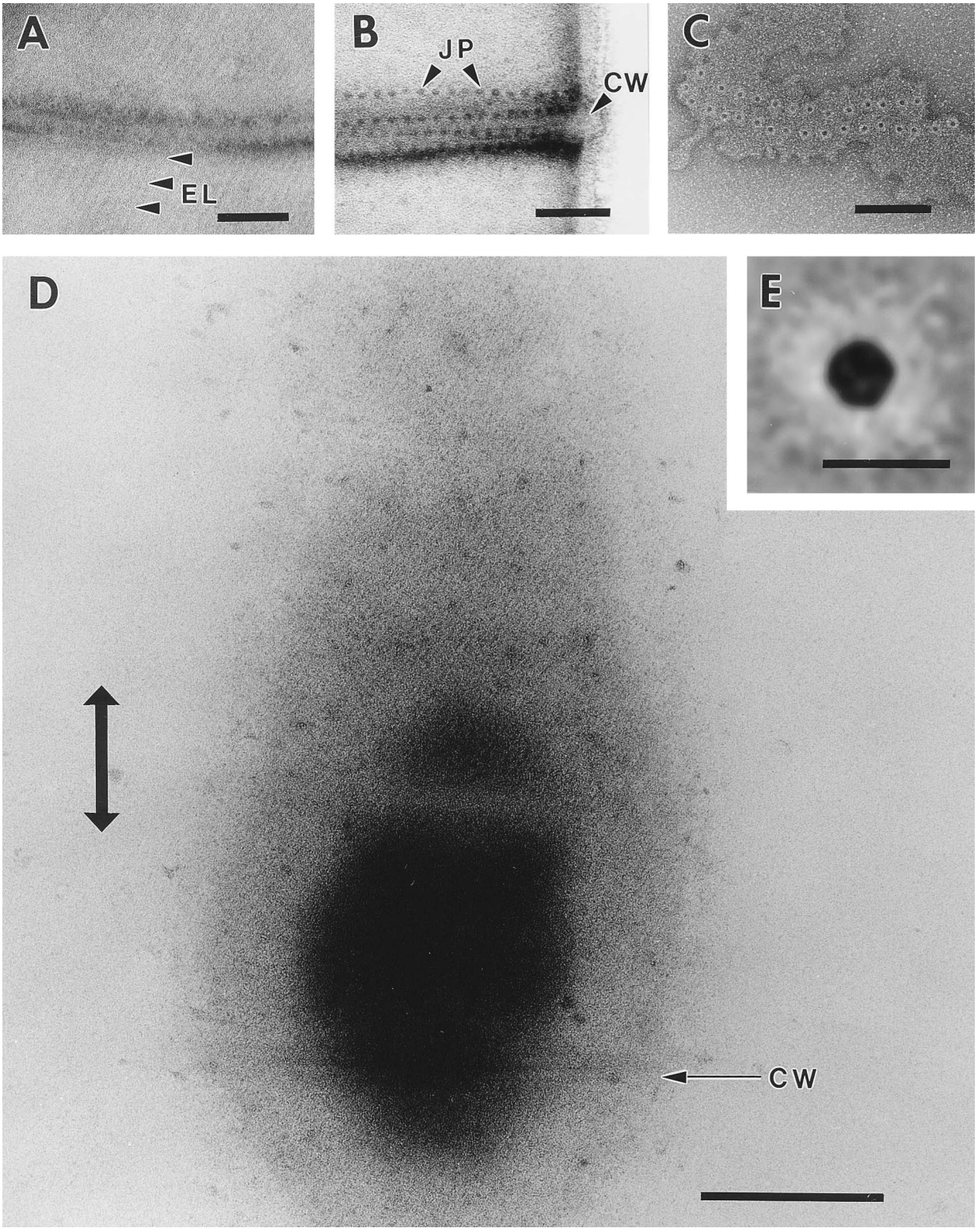

FIG. 3. (A) *P. uncinatum* (strain Baikal). Isolated cell wall with the outer membrane and the serrated external layer (EL) still attached. On both sides of the cross wall, the ring-shaped counterparts of the junctional pores with their central pores are visible. Bar, 150 nm. (B) *P. uncinatum* (strain Baikal). Isolated murein sacculi with the negative stained junctional pores (JP). CW, cross wall. Bar, 150 nm. (C) *P. uncinatum* (strain Baikal). Isolated outer membrane patch with the ring-shaped counterparts of the JP. Bar, 150 nm. (D) *P. uncinatum* (strain Tübingen). Tangential section of a motile filament showing the helical, clockwise arrangement of the EL. The secreted slime is not preserved. The large arrow indicates the long axis of the filament. Bar, 250 nm. (E) *P. uncinatum* (strain Baikal). Average of 237 ring-shaped counterparts of the JP. Bar, 10 nm.

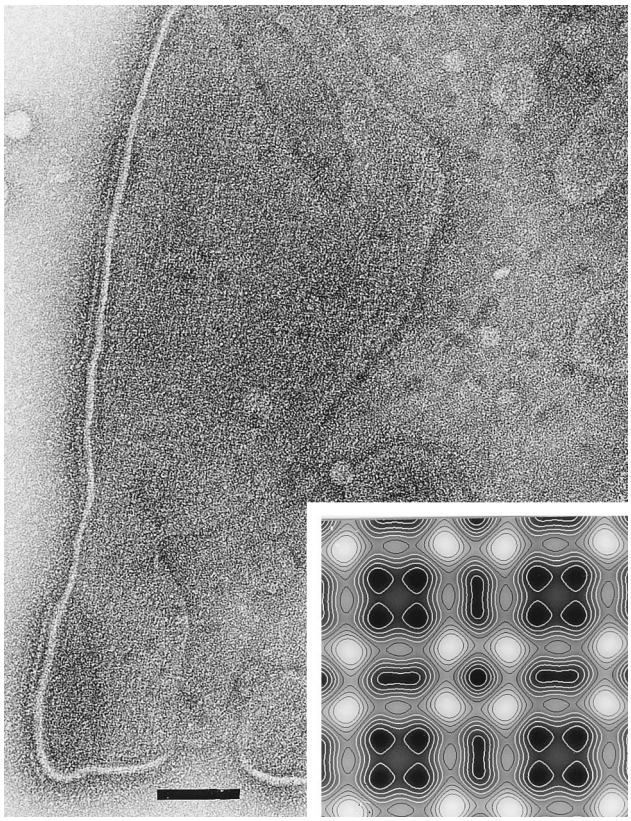

FIG. 4. *P. uncinatum* (strain Baikal). Isolated cell wall with a large patch of the p4 symmetric S-layer still attached to the outer membrane. Bar, 100 nm. The inset shows a two-dimensional reconstruction of the S-layer, based upon the micrograph. Lattice constant, 11.2 nm.

sions were very similar in all the species. In negatively stained, isolated outer membranes, a ring-like structure was found (Fig. 3C and E). These ring structures consisted of a less-electron-dense peripheral zone, 14 to 16 nm in diameter, and a central opaque core structure of 7 to 8 nm. These ring structures are very similar to the "perforations" of cyanobacterial cell walls described by Guglielmi and Cohen-Bazire (19). As the diameter, center-to-center spacing, number, and location at the cross wall of this complex ring structure match the dimensions and the arrangement of the junctional pores, the ring structures seem to be the structural counterparts of the junctional pores in the outer membrane (Fig. 3A, B, and C).

Images of septa in different states of development clearly show the formation of the channels of the junctional pores (Fig. 1E and 2E). Interestingly, the junction of the outer membrane is not the initial site of development. As in other cyanobacteria (28), the formation of the pore channels starts on the cytoplasmic side of the peptidoglycan. As the cross wall grows, the channels become deeper. The circumferential membrane junction (Fig. 1E and F) is not established until the pores span the whole peptidoglycan.

Surface structures. All the species possess additional layers on the top of the outer membrane which are 11 to 20 nm thick in cryopreparations (Fig. 1A to F). The external surface shows serrated structures of between 4.5 nm and 6.5 nm in height and having a width at the base of up to 12 nm. Electron microscopy of negatively stained isolated cell walls revealed that the complex layer consists of a tetragonal S-layer (Fig. 4) together with a tightly bound fibrillar array which forms the serrated structures in cross sections and is regular but apparently not crystalline.

In some filaments, fuzzy or hair-like fibers are visible radiating outwards from the external layer surface (Fig. 1A). In both *Phormidium* strains and *L. aeruginosa*, the fibers had maximum lengths of 20 to 30 nm, while those in *O. princeps* were 17 to 50 nm. Whether these fibers represent an early stage of the development of the sheath is not yet clear. In tangential sections, the serrated structures (with or without fibers) run in parallel and form helical arrays around the trichome surface with a pitch of $65 \pm 3°$ in all the species. The orientation of these periodic surface fibrils corresponds to the sense of rotation of the organism during the gliding movement. In *O. princeps* and *L. aeruginosa*, which rotate counterclockwise, the arrangement is counterclockwise (Fig. 2C and D), while in all the other species, the rotation is clockwise, as is the arrangement of the surface fibrils (Fig. 3D). We were unable to detect any further structures on the filament surface or within the cell wall which had features suggesting a relationship with the mode of movement.

Ultrastructure of the slime and the sheath. Even with cryosubstitution, the extracellular slime was either barely or not preserved at all, except for those of the *Phormidium* strain Tübingen and *L. aeruginosa*, for which a high concentration of OsO_4 (4% or more) allowed them to be preserved. The slime tube, which is shed behind the trichome (Fig. 5A and B), is between 10 and 50 nm thick and composed of fine, more or less parallel fibrils with diameters of 4 to 6 nm. The orientation of these slime fibrils corresponds to the orientation of the surface fibrils. This coincidence is very strong in the contact zone between the slime and the surface fibrils and becomes less pronounced in the outer part of the slime tube (Fig. 6A and B). If the slime is secreted in minimal amounts by the filament, this slime moves along the surface of the stationary filament in helical bands (Fig. 2A). By comparison, highly motile filaments glide through an elastic slime tube (Fig. 5A) which is left behind as a collapsed and twisted trail (Fig. 5B).

The sheaths of the nonmotile trichomes were always preserved, although these structures often show some structural disintegration (Fig. 1D). In accordance with earlier findings (27), we found that in the counterclockwise-rotating *O. princeps* (Fig. 2B) and *L. aeruginosa*, the sheath fibrils form a left-handed helix, while they form a right-handed helix in the clockwise-rotating *Phormidium* strains (data not shown). Therefore, the orientations of the sheath fibrils and the surface fibrils of the serrated external layers were identical.

Freeze fracturing and freeze etching provided further structural information. Arrays seen on the surfaces of the cells showed the helically arranged surface fibrils with diameters of 8 to 12 nm. In all the species, the trichome surfaces were covered with slime, composed of fine fibrils which run parallel to the external surface fibrils (data not shown).

DISCUSSION

While most theories about the gliding movement of cyanobacteria assume a mechanical interaction between the cell surface and the substrate, it is still a matter of controversy how the moving force is generated in the shearing zone. Two favorably suggested mechanisms are submicroscopical contraction waves of helical fibrils below the outer membrane (23) and the extrusion of slime which pushes the filament forward (6, 42).

The careful reinvestigation of the cell envelope of *O. princeps* by cryotechniques did not reveal any fibrillar structures underneath the outer membrane as described by Halfen (21).

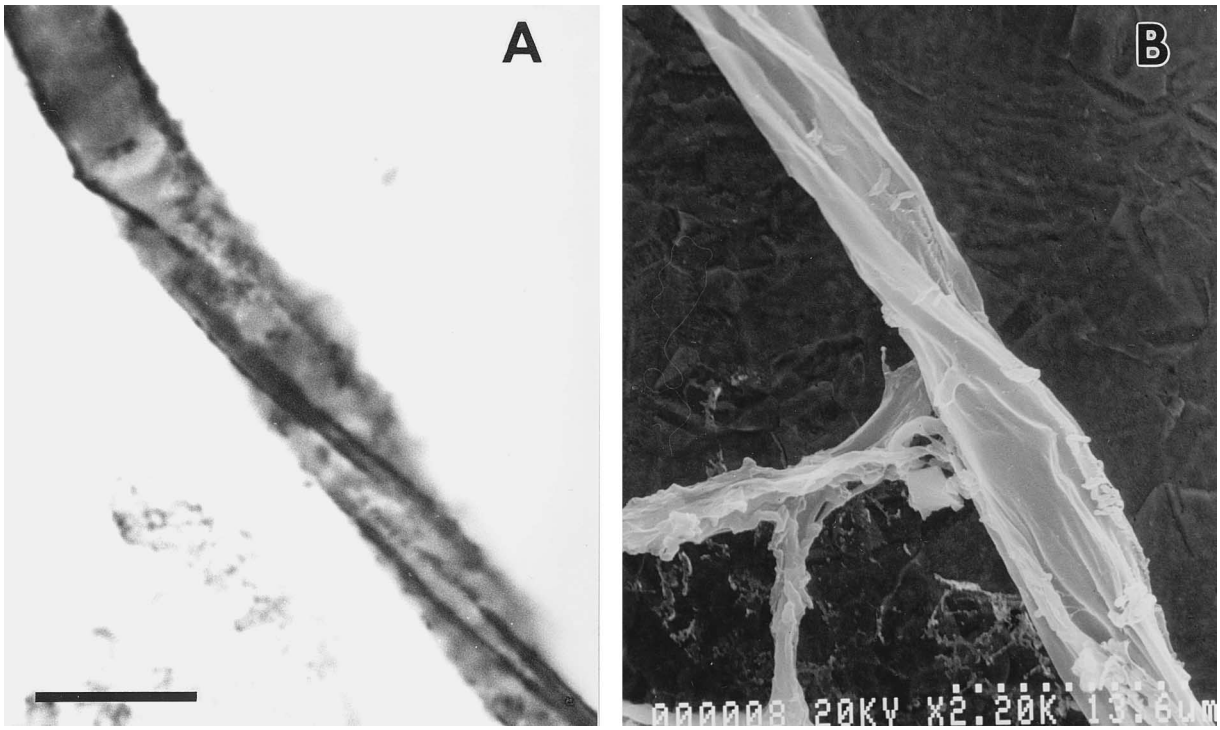

FIG. 5. (A) Light micrograph of a rapidly gliding *L. aeruginosa* filament leaving behind its slime tube, which is stained with India ink particles that are sticking to the mucus. The image is reversed to show the arrangement with respect to the filament. Bar, 10 μm. (B) Scanning electron micrograph of a collapsed slime tube behind an *L. aeruginosa* filament. As a result of the friction between the slime and the filament surface during rotation, the tube is folded with respect to the long axis of the filament.

As the circumferential junctions partition the periplasmic space between the peptidoglycan and the outer membrane at every septum, this is not a continuous compartment along the whole filament. It is therefore unlikely that fibrils with diameters of 5 to 8 nm could run along the entire length of the filament in the space beneath the outer membrane. Instead, it now seems likely that the helically arranged surface fibrils which create the serrated appearance in cross sections correspond to the formerly described "fibrils just under the outer membrane" (22), except for their location.

The whole complex external surface layer is formed by two different structural elements (Fig. 7): a tetragonal S-layer anchored to the outer membrane and a parallel array of helically arranged surface fibrils with a regular spacing of 14 nm on top of the S-layer. The presence of an S-layer in gliding filamentous cyanobacteria is surprising (44). So far, S-layers have not been observed in gliding bacteria, with the exceptions of *Flexibacter polymorphus* (41) and *Thioploca*, *Beggiatoa* (34, 45), and *Herpetosiphon* spp. (39). Only the *Flexibacter* and *Beggiatoa* layers have been described in some detail. The former consisted of closely packed goblet-shaped particles, while the latter possessed longitudinal surface fibrils that strongly resemble the surface fibrils described in this study.

A striking observation is that the orientation of the surface fibrils of the external layers is correlated with the screw-like motion of the filaments. As the helical surface fibrils represent the shear zone of the filament, they might play an important role in the process of gliding. This role could be either an active one, i.e., the fibrils act as a contractile motor, or a passive one, i.e., they provide a screw thread structure guiding the rotation of the trichome.

We hypothesize that the extrusion of slime, which moves relative to the helical surface fibrils, should create sufficient power to drive the trichome forward and thereby promote the rotational movement. The alternative possibility, that the surface fibrils are themselves the contractile motor, seems for us unlikely because of the fact that contractile processes are energy dependent and have to be driven by ATP or by a proton gradient across the cytoplasmic membrane. The position of the S-layer–surface-fibril complex outside the outer membrane appears to be too far away from the cytoplasmic membrane to permit such an energy supply. In addition, none of the S-layers studied so far are energy-controlled structures (43). Taking all these observations into account, an active role for the S-layer–surface-fibril assembly is hardly imaginable.

A prerequisite for the hypothesis of a passive screw thread function of the surface fibrils would be that the interaction has appropriate physicochemical properties (12). The electron microscopical images clearly demonstrate that the slime layer does not extend more than several nanometers beyond the serrated surface fibrils (Fig. 1). The images also show an identical orientational arrangement, especially at the inner contact zone (Fig. 6). The appropriate physicochemical properties mean that the interaction of the slime, the surface fibrils, and the substratum allows translational motion along the surface fibrils but not along the substratum. Similar temporary adhesive properties have been demonstrated for the slime of *Flexibacter* isolates (25) and would also explain the observed movements of particles sticking to the mucus (6, 42).

A rough estimate of the amount of extruded mucilage shows that only about 5% of the metabolic activity of motile cells is required. While the total increase of biomass in *Phormidium* cultures (strain Baikal) at exponential growth was about 3.7 mg of dry weight per petri dish per day, within the same time, the

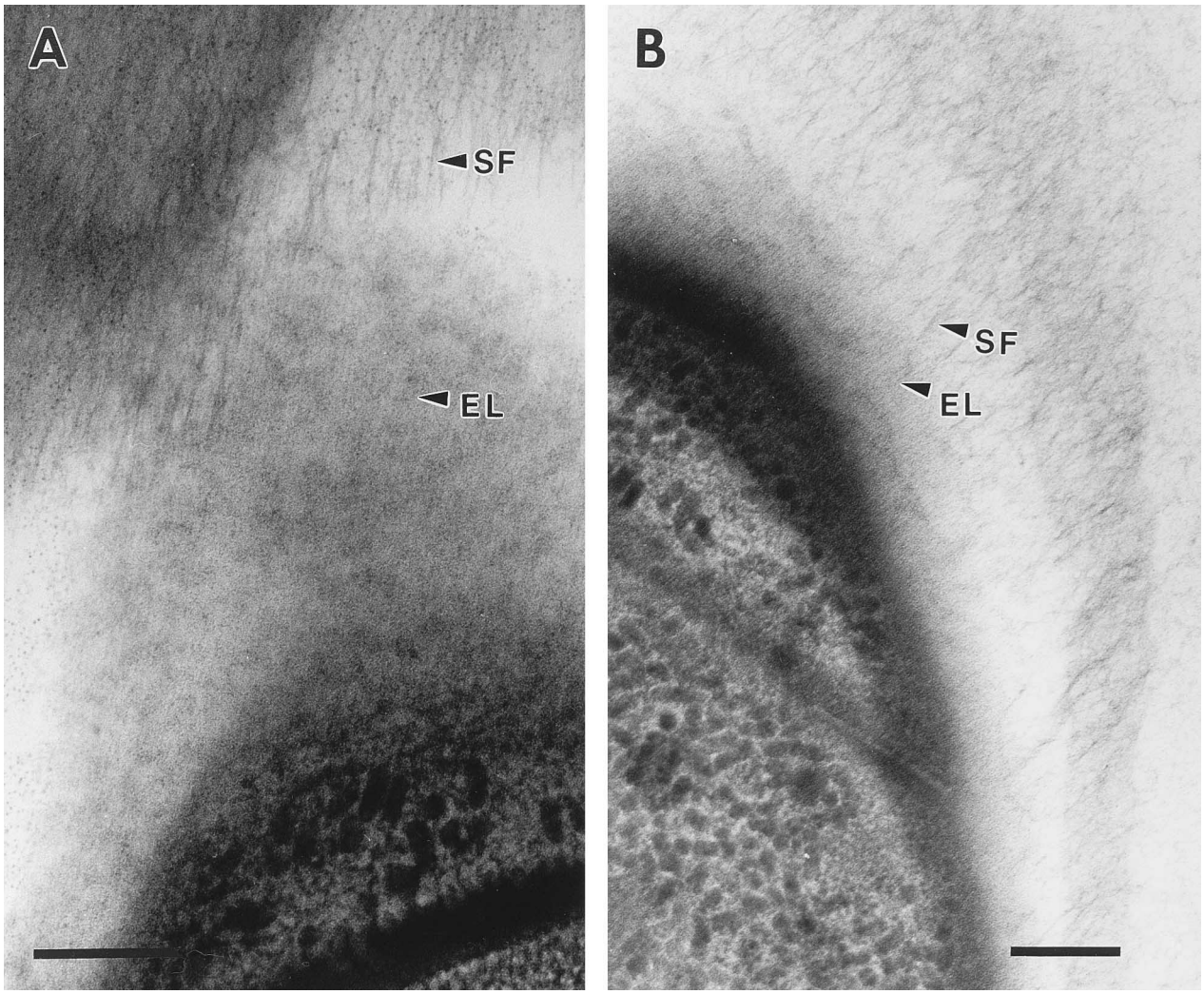

FIG. 6. (A) *P. uncinatum* (strain Tübingen). Grazing surface section of a highly motile filament with the preserved slime fibrils (SF). The arrangement of the serrated surface fibrils (EL) and the SF is identical. Bar, 200 nm. (B) *P. uncinatum* (strain Tübingen). Grazing surface section of a highly motile filament with the SF. The arrangements of the EL and the SF are identical. Bar, 200 nm.

produced biomass of slime was only about 175 μg. Certainly, this calculation is not very accurate, but it does not seem to be an unreasonable estimate.

Although the topography of the cell surface could explain the helical movement, one observation is still difficult to explain: the direction of movement in members of the *Oscillatoriaceae* frequently changes. These reversals indicate that the motor is able to switch or that the direction of extrusion has to switch. Structures which could fulfill these requirements are the junctional pores which point in opposite directions at the cross walls of neighboring cells. If only those pores in all the cells of the filament which are directed to the same pole of the trichome secrete slime, a directed movement forward or backward will result. So far, we have only indications that the junctional pores are involved in slime extrusion, as the pore channels are filled with electron-dense material in motile filaments but are empty in nonmotile ones. However, the junctional pores seem to be the only place where a rapid extrusion of slime could be possible. They are the only identically arranged ring-like structures located in the outer membrane which might facilitate slime extrusion. Interestingly, the ap-

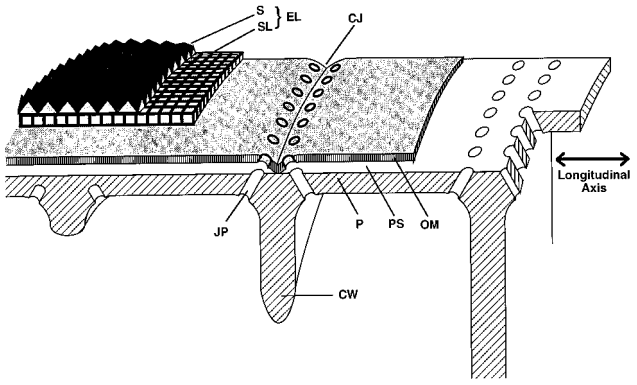

FIG. 7. A schematic diagram showing the cell wall structure of the gliding members of the *Oscillatoriaceae*. The orientation of the serrated surface of the external layer varies, depending on the sense of revolution of the filament during gliding. CW, cross wall; CJ, circumferential junction; EL, external layer; JP, junctional pore with its counterpart in the outer membrane; OM, outer membrane; P, peptidoglycan; PS, periplasmic space; S, serrated surface of the external layer; SL, tetragonal S-layer.

pearance of these outer membrane structures shows a high similarity with that of pores in *Acetobacter xylinum* (49), in which the pores are the export sites of cellulose fibers (1).

The idea of jet propulsion as the basis for gliding motility has always evoked controversy. It should be emphasized that the slime is not propelled out at one end, with the effect that the filament is moved in the opposite direction. If this were true, the filaments should also move freely when suspended in the medium, which has never been observed. Indeed, we believe that the proximity of the filament surface, the slime, and the substratum will create shear forces sufficiently large to move the organism.

Although we can now correlate gliding in members of the *Oscillatoriaceae* with certain surface structures, we are of course far from a full understanding of the complex mechanism of gliding. The isolation and biochemical characterization of the S-layer and the surface fibrils as well as a more elaborate examination of the slime extrusion process have to be carried out in order to reach a more complete understanding of the gliding process. Further investigations should also clarify whether highly ordered surface structures (like in the abovementioned species) are common features of the cell walls of gliding bacteria.

ACKNOWLEDGMENTS

We thank W. Nultsch (University of Marburg) for providing the *Phormidium* strain Tübingen and V. Donkor (University of Erlangen) for *Phormidium* strain Baikal. We also thank Robert M. Glaeser and Harald Engelhardt for critical reading of the manuscript and Toni Hillebrand for drawing the cell wall scheme.

One of the authors (E.H.) was the recipient of a grant from the Studienstiftung des Deutschen Volkes.

REFERENCES

1. **Brown, R. M., Jr., J. H. M. Willison, and C. M. Richardson.** 1976. Cellulose biosynthesis in *Acetobacter xylinum*: visualization of the site of synthesis and direct measurement of the in vivo process. Proc. Natl. Acad. Sci. USA **73:**4565–4569.
2. **Burchard, A. C., R. P. Burchard, and J. A. Kloetzel.** 1977. Intracellular, periodic structures in the gliding bacterium *Myxococcus xanthus*. J. Bacteriol. **132:**666–672.
3. **Burchard, R. P.** 1981. Gliding motility. Annu. Rev. Microbiol. **35:**497–529.
4. **Burkholder, P. R.** 1934. Movement in Cyanophyceae. Q. Rev. Biol. **9:**438–459.
5. **Castenholz, R. W.** 1969. Thermophilic blue-green algae and the thermal environment. Bacteriol. Rev. **33:**476–504.
6. **Drews, G., and W. Nultsch.** 1962. Spezielle Bewegungsmechanismen von Einzellern (Bakterien, Algen), p. 887–894. *In* W. Ruhland (ed.), Handbuch der Pflanzenphysiologie, Vol. 17/2. Springer Verlag, Berlin.
7. **Drews, G., and J. Weckesser.** 1982. Function, structure and composition of cell walls and external layers, p. 333–357. *In* N. G. Carr and B. A. Whitton (ed.), The biology of cyanobacteria. Blackwell Scientific Publications, Oxford.
8. **Dubochet, J., J. Lepault, R. Freeman, J. A. Berriman, and J.-C. Homo.** 1982. Electron microscopy of frozen water and aqueous solutions. J. Microsc. **128:**219–237.
9. **Dworkin, M.** 1966. Biology of the myxobacteria. Annu. Rev. Microbiol. **20:**75–106.
10. **Dworkin, M., K. H. Keller, and D. Weisberg.** 1983. Experimental observations consistent with a surface tension model of gliding motility of *Myxococcus xanthus*. J. Bacteriol. **155:**1367–1371.
11. **Escaig, J.** 1982. New instruments which facilitate rapid freezing at 83°K and 6°K. J. Microsc. **126:**221–229.
12. **Fattom, A., and M. Shilo.** 1984. Hydrophobicity as an adhesion mechanism of benthic cyanobacteria. Appl. Environ. Microbiol. **47:**135–143.
13. **Fritsch, F. E.** 1945. The structure and reproduction of the algae, vol. II, p. 800–804. Cambridge University Press, Cambridge.
14. **Glagoleva, T. N., A. N. Glagolev, M. V. Gusev, and K. A. Nikitina.** 1980. Proton motive force supports gliding in cyanobacteria. FEBS Lett. **117:**49–53.
15. **Golecki, J. R.** 1977. Studies on ultrastructure and composition of cell walls of the cyanobacterium *Anacystis nidulans*. Arch. Microbiol. **114:**35–41.
16. **Graham, L. L.** 1992. Freeze-substitution studies of bacteria. Electron Microsc. Rev. **5:**77–103.
17. **Graham, L. L., and T. J. Beveridge.** 1990. Evaluation of freeze-substitution and conventional embedding protocols for routine electron microscopic processing of eubacteria. J. Bacteriol. **172:**2150–2159.
18. **Graham, L. L., R. Harris, W. Villiger, and T. J. Beveridge.** 1991. Freeze-substitution of gram-negative eubacteria: general cell morphology and envelope profiles. J. Bacteriol. **173:**1623–1633.
19. **Guglielmi, G., and G. Cohen-Bazire.** 1982. Structure et distribution des pores et des perforations de l'enveloppe de peptidoglycane chez quelques cyanobactéries. Protistologica **18:**151–165.
20. **Häder, D.-P., and E. Hoiczyk.** 1992. Gliding motility, p. 1–38. *In* M. Melkonian (ed.), Algal cell motility. Chapman and Hall, New York.
21. **Halfen, L. N.** 1973. Gliding motility in *Oscillatoria*: ultrastructural and chemical characterization of the fibrillar layer. J. Phycol. **9:**248–253.
22. **Halfen, L. N.** 1979. Gliding movements, p. 250–269. *In* W. Haupt and M. E. Feinleib (ed.), Encyclopedia of plant physiology, new series vol. 7. Springer Verlag, Berlin.
23. **Halfen, L. N., and R. W. Castenholz.** 1971. Gliding in a blue-green alga *Oscillatoria princeps*. J. Phycol. **7:**133–145.
24. **Hobot, J. A., E. Carlemalm, W. Villiger, and E. Kellenberger.** 1984. Periplasmic gel: new concept resulting from the reinvestigation of bacterial cell envelope ultrastructure by new methods. J. Bacteriol. **160:**143–152.
25. **Humphrey, B. A., M. R. Dickson, and K. C. Marshall.** 1979. Physicochemical and in situ observations on the adhesion of gliding bacteria to surfaces. Arch. Microbiol. **120:**231–238.
26. **Lamont, H. C.** 1969. Sacrificial cell death and trichome breakage in an *Oscillatoriacean* blue-green alga: the role of murein. Arch. Microbiol. **69:** 237–259.
27. **Lamont, H. C.** 1969. Shear-oriented microfibrils in the mucilaginous investments of two motile oscillatoriacean blue-green algae. J. Bacteriol. **97:**350–361.
28. **Lang, N. J.** 1977. *Starria zimbabweensis* (Cyanophyceae) gen. nov. et sp. nov.: a filament triradiate in transverse section. J. Phycol. **13:**288–296.
29. **Lapidus, I. R., and H. C. Berg.** 1982. Gliding motility of *Cytophaga* sp. strain U67. J. Bacteriol. **151:**384–398.
30. **Luft, J. H.** 1971. Ruthenium red and violet. I. Chemistry, purification, methods for use for electron microscopy and mechanism of action. Anat. Rec. **171:**347–368.
31. **Lünsdorf, H., and R. Reichenbach.** 1989. Ultrastructural details of the apparatus of gliding motility of *Myxococcus fulvus* (*Myxobacterales*). J. Gen. Microbiol. **135:**1633–1641.
32. **MacAlister, T. J., B. MacDonald, and L. I. Rothfield.** 1983. The periseptal annulus: an organelle associated with cell division in gram-negative bacteria. Proc. Natl. Acad. Sci. USA **80:**1372–1376.
33. **MacRae, T. H., and H. D. McCurdy.** 1976. Evidence for motility-related fimbriae in the gliding microorganism *Myxococcus xanthus*. Can. J. Microbiol. **22:**1589–1593.
34. **Maier, S., and R. G. E. Murray.** 1965. The fine structure of *Thioploca ingrica* and a comparison with *Beggiatoa*. Can. J. Microbiol. **11:**645–655.
35. **Nultsch, W.** 1962. Der Einfluß des Lichtes auf die Bewegung der Cyanophyceen. III. Photophobotaxis bei *Phormidium uncinatum*. Planta **58:**647–663.
36. **Nultsch, W., and D.-P. Häder.** 1974. Über die Rolle der beiden Photosysteme in der Photophobotaxis von *Phormidium uncinatum*. Ber. Dtsch. Bot. Ges. **87:**83–92.
37. **Pate, J. L., and L. Y. E. Chang.** 1979. Evidence that gliding motility in prokaryotic cells is driven by rotary assemblies in the cell envelopes. Curr. Microbiol. **2:**59–64.
38. **Pringsheim, E. G.** 1951. The *Vitreoscillaceae*: a family of colourless, gliding filamentous organisms. J. Gen. Microbiol. **5:**124–149.
39. **Reichenbach, H., and J. R. Golecki.** 1975. The fine structure of *Herpetosiphon*, and a note on the taxonomy of the genus. Arch. Microbiol. **102:**281–291.
40. **Reynolds, E. S.** 1963. The use of lead citrate at high pH as an electron-opaque stain in electron microscopy. J. Cell Biol. **17:**208–212.
41. **Ridgway, H. F., R. M. Wagner, W. T. Dawsey, and R. A. Lewin.** 1975. Fine structure of the cell envelope layers of *Flexibacter polymorphus*. Can. J. Microbiol. **21:**1733–1750.
42. **Schulz, G.** 1955. Bewegungsstudien sowie elektronenmikroskopische Membranuntersuchungen an Cyanophyceen. Arch. Mikrobiol. **21:**335–370.
43. **Sleytr, U. B., and P. Messner.** 1983. Crystalline surface layers on bacteria. Annu. Rev. Microbiol. **37:**311–339.
44. **Smarda, J.** 1988. S-layers in cyanobacteria, p. 127–132. *In* U. B. Sleytr, P. Messner, D. Pum, and M. Sara (ed.), Crystalline bacterial cell surface layers. Springer Verlag, Berlin.
45. **Strohl, W. R., S. H. Karen, and J. M. Larkin.** 1982. Ultrastructure of *Beggiatoa alba* strain B15LD. J. Gen. Microbiol. **128:**73–84.
46. **Thomas, E. A.** 1970. Beobachtungen über das Wandern von *Phormidium autumnale*. Schweiz. Z. Hydrol. **32:**523–531.
47. **Van Eykelenburg, C.** 1977. On the morphology and ultrastructure of the cell wall of *Spirulina platensis*. Antonie Leeuwenhoek **43:**89–99.
48. **Weckesser, J., and U.-J. Jürgens.** 1988. Cell walls and external layers. Methods Enzymol. **167:**173–188.
49. **Zaar, K.** 1979. Visualization of pores (export sites) correlated with cellulose production in the envelope of the gram-negative bacterium *Acetobacter xylinum*. J. Cell Biol. **80:**773–777.